



Contents lists available at ScienceDirect

Journal of Plant Physiology

journal homepage: www.elsevier.de/jplph



Disarrangement of actin filaments and Ca^{2+} gradient by CdCl_2 alters cell wall construction in *Arabidopsis thaliana* root hairs by inhibiting vesicular trafficking

Jun-Ling Fan^{a,b}, Xue-Zhi Wei^b, Li-Chuan Wan^a, Ling-Yun Zhang^c, Xue-Qin Zhao^{a,b}, Wei-Zhong Liu^b, Huai-Qin Hao^a, Hai-Yan Zhang^{a,*}

^a Key Laboratory of Photosynthesis and Molecular Environmental Physiology, Institute of Botany, Chinese Academy of Sciences, Xiangshan, Beijing 100093, China

^b College of Life Sciences, Shanxi Normal University, Linfen 041000, China

^c Key Laboratory of Forest Silviculture and Conservation of the Ministry of Education, Beijing Forestry University, Beijing 100083, China

ARTICLE INFO

Article history:

Received 21 July 2010

Received in revised form 3 January 2011

Accepted 27 January 2011

Keywords:

Actin filaments

Ca^{2+} gradient

Cadmium

Cell wall

Root hair

ABSTRACT

Cadmium (Cd), one of the most toxic heavy metals, inhibits many cellular and physiological processes in plants. Here, the involvement of cytoplasmic Ca^{2+} gradient and actin filaments (AFs) in vesicular trafficking, cell wall deposition and tip growth was investigated during root (hair) development of *Arabidopsis thaliana* in response to CdCl_2 treatment. Seed germination and root elongation were prevented in a dose- and time-dependent manner by CdCl_2 treatment. Fluorescence labelling and non-invasive detection showed that CdCl_2 inhibited extracellular Ca^{2+} influx, promoted intracellular Ca^{2+} efflux, and disturbed the cytoplasmic tip-focused Ca^{2+} gradient. *In vivo* labelling revealed that CdCl_2 modified actin organization, which subsequently contributed to vesicle trafficking. Transmission electron microscopy revealed that CdCl_2 induced cytoplasmic vacuolization and was detrimental to organelles such as mitochondria and endoplasmic reticulum (ER). Finally, immunofluorescent labelling and Fourier transform infrared (FTIR) analysis indicated that configuration/distribution of cell wall components such as pectins and cellulose was significantly altered in response to CdCl_2 . Our results indicate that CdCl_2 induces disruption of Ca^{2+} gradient and AFs affects the distribution of cell wall components in root hairs by disturbing vesicular trafficking in *A. thaliana*.

© 2011 Elsevier GmbH. All rights reserved.

Introduction

Along with worldwide industrial development, the production of heavy metals has increased rapidly. Heavy metals affect numerous metabolic and/or developmental processes in all living organisms. Cadmium (Cd) is one of the most toxic non-essential heavy metals and has become a major environmental pollutant. A high concentration of Cd can induce carcinogenic, mutagenic, and teratogenic effects in a large number of animal species. In plant cells, Cd can affect many vital processes, for example, it inhibits root growth and reduces fresh biomass, changes morphology, and causes increased activity of antioxidant enzymes (Zhang et al., 2005; Verma et al., 2008). As for mechanisms of Cd toxicity in plant cells, various prospective intracellular targets for Cd have been discussed. It is well known that Cd has a high affinity for sulphhydryl groups of proteins and thereby inhibits SH-bearing,

redox-regulated enzymes in many cellular processes (Hall, 2002). Cd also binds to calmodulin, activates it, and plays an important role in Ca-dependent regulatory pathways (Powlin et al., 1997). Furthermore, the displacement of other divalent cat ions such as Zn and Fe from proteins causes the release of “free” ions that can lead to oxidative injury via free Fe/Cu-catalyzed Fenton reactions (Stohs et al., 2000).

The cell wall is the first barrier to metal ion uptake in higher plants. This extracellular barrier has the capacity to bind metal ions in negatively charged sites. When exposed to a heavy metal environment, the cell wall composition changes dramatically. Garcia-Rios et al. (2007) reported that both insoluble polysaccharides and polysaccharide sulphate content in the cell wall exhibit evident differences between two red macroalgal species in response to Cd exposure. The roles of polysaccharides in cell walls during metal ion accumulation and heavy metal tolerance have been described by several researchers (Raize et al., 2004; Mikes et al., 2005). There has also been report on the inhibition of some cell wall enzyme activities (e.g. peroxidase, NADH oxidase, and IAA oxidase) after Cd treatment (Chaoui and El Ferjani, 2005). However, few studies have investigated *in situ* the alteration of cell wall components, e.g. pectin and cellulose, after Cd application.

* Corresponding author. Tel.: +86 10 62836206; fax: +86 10 62836211.

E-mail addresses: junlingfan@163.com (J.-L. Fan), wxz328@sohu.com (X.-Z. Wei), wanlichuan@ibcas.ac.cn (L.-C. Wan), lyzhang73@sohu.com (L.-Y. Zhang), zhaoyuanli123@yahoo.com.cn (X.-Q. Zhao), liuweizh@dns.sxtu.edu.cn (W.-Z. Liu), hqhao@ibcas.ac.cn (H.-Q. Hao), hyz@ibcas.ac.cn (H.-Y. Zhang).

Materials involved in constructing the cell wall come from secretory vesicles that accumulate beneath the plasma membrane and undergo fusion with the plasma membrane in fast-growing cells (Ovecka et al., 2005; Bove et al., 2008). Many cellular elements are considered crucial molecular players in triggering these fusion events, such as the Ca^{2+} gradient, actin cytoskeleton, and intracellular signal transduction (Lee et al., 2008; Vassilieva and Nusrat, 2008), and a variety of stimuli can influence the dynamics of these elements. For example, NaCl stress can reduce the magnitude of the Ca^{2+} gradient in the apex of root hairs in *Arabidopsis thaliana*, and cold shock results in a dramatic increase of $[\text{Ca}^{2+}]_{\text{cyt}}$ and simultaneous disruption of microtubules and microfilaments (Orvar et al., 2000; Halperin et al., 2003). However, few studies have been published on the effects of Cd stress on Ca level, actin filament (AF) arrangement, and cell wall composition of plant cells *in vivo* and *in situ*. Furthermore, the cellular mechanism involved in cell wall alterations induced by Cd has not yet been elucidated.

The root hair, a typical tip-growth cell, as well as rhizoids, leaf hairs, and pollen tubes, are widely used as suitable experimental systems for investigation of the Ca^{2+} gradient, cytoskeletal dynamics, and cell wall construction (Baluska et al., 2000). These tissues are soft, originate from specific epidermal cells, and undergo a highly polarized expansion of the cell wall at the extreme tip. Such a cylindrical cell is thought to be very sensitive to environmental stimuli and relatively easy to analyze during morphogenesis. Moreover, being a major organ of plant seedlings for metal uptake from medium makes the root hair a suitable system for toxicity studies.

In this work, we show that Cd stress modulates root development, including root growth, Ca^{2+} gradient, AFs organization, vesicular trafficking, and cell wall formation, in *A. thaliana*. Our results indicate that Cd might affect cell wall construction by disturbing the Ca^{2+} gradient and actin cytoskeleton, thus inhibiting vesicular trafficking in root hairs.

Materials and methods

Plant material and cultivation

All *Arabidopsis thaliana* used were in the Columbia background. Seeds were surface-sterilized and germinated on 1/2 Murashige and Skoog medium (Sigma) supplemented with 1% (w/v) sucrose, 1% (w/v) agar, and the indicated concentrations of CdCl_2 at 22 °C under continuous light. Twelve- and 3-day-old seedlings were chosen for root length measurement and for other experiments, respectively. For seed germination rate analysis and root length measurement, the number of seeds and seedlings examined was at least 200 and 30 for each treatment. For microscopic observation, at least 5–10 root hairs which grew normally were selected for measurement in each treatment at each time. All experiments were performed in triplicate.

Fluo-4/AM loading and confocal imaging of cytoplasmic Ca^{2+}

Fluo-4/AM ester was loaded into root hairs at low temperature (4 °C) in the dark at a final concentration of 10 μM as described previously (Zhang et al., 1998). After a 2-h incubation, the root hairs were washed with standard medium several times and left at room temperature for 1 h. The samples were mounted and photographed with a Zeiss LSM 510 META CLSM (Zeiss Co., Germany). Fluorescence was detected using 488 nm excitation and 505–530 nm band pass filter.

Measurement of root hair tip extracellular Ca^{2+} fluxes

Net Ca^{2+} fluxes were measured using the scanning ion-selective electrode technique (SIET) as described previously (Holdaway-Clarke et al., 1997), with small modifications, in Xu-Yue (Science and Technology Co. Ltd., Beijing, China, www.xuyue.net). Ca^{2+} -selective microelectrodes with an external tip diameter of approximately 3 μm were manufactured and salinized with tributylchlorosilane, and the tips were backfilled with commercially available ion-selective cocktails (Ca Ionophore I – Cocktail A, 21048, Fluka, Busch, Switzerland). The self-referencing vibrating probe oscillated with an excursion of 10 μm , completing a whole cycle in about 5.72 s. Root hairs selected for measurement were growing normally. All experiments were repeated three times, and Ca^{2+} fluxes of at least five root hairs were measured in each treatment at each time. The obtained data were analysed in an Excel spreadsheet to convert data from the background-mV estimation of concentration and microvolt difference estimation of the local gradient into specific ion influx ($\text{pmol cm}^{-2} \text{ s}^{-1}$).

Confocal imaging of actin in root hairs

Seedlings containing FABD2-GFP were mounted in 1/2 Murashige and Skoog medium with indicated CdCl_2 concentration and incubation time. Photos were taken with a Zeiss LSM 510 META CLSM (Zeiss Co., Germany). FABD2-GFP was excited using the 488 nm line of an argon ion laser and fluorescence emission was collected using 505–530 nm band pass filter.

FM4-64 staining to analyze vesicular trafficking in the apex of root hairs

Loading of cells with FM4-64 dye was generally achieved by direct application to growing root hairs. Fluorescence from FM4-64 staining was detected using LSCM (laser scanning confocal microscopy). FM4-64 was excited with 488 nm and emission was detected using 575–615 nm band pass filter. Serial optical sections were made every 30 s for about 60 images 2–3 min after dye application until the fluorescence finally reached saturation.

Immunolabelling of pectins in root cell walls

Immunolabelling of pectins in the root cell wall was carried out following the procedures described by Willats et al. (2001). The primary antibodies were used at 1:50 dilution. Fluorescein isothiocyanate (FITC)-conjugated anti-rat IgG was diluted at 1:50. Seedlings were mounted and photographed using LSCM. FITC was excited at 488 nm and detected by 505–530 nm band pass filter. Controls were prepared by omitting the primary antibody.

Fourier transform infrared analysis of the root hair cell wall

Seedlings were washed three times with deionized water, and then dried in a layer on a barium fluoride window (13 mm diameter \times 2 mm thick). Spectra were obtained from the tip region of root hairs with a MAGNA 750 Fourier transform infrared (FTIR) spectrometer (Nicolet Corp., Tokyo, Japan) equipped with a mercury–cadmium–telluride detector. Spectra were obtained at a resolution of 8 cm^{-1} , with 128 co-added interferograms, and normalized to obtain relative absorbance as described previously (Chen et al., 2007).

Electron microscopy

For electron microscopy, seedlings of *A. thaliana* were fixed for 4 h in 2.5% glutaraldehyde and 3% paraformaldehyde in 100 mM

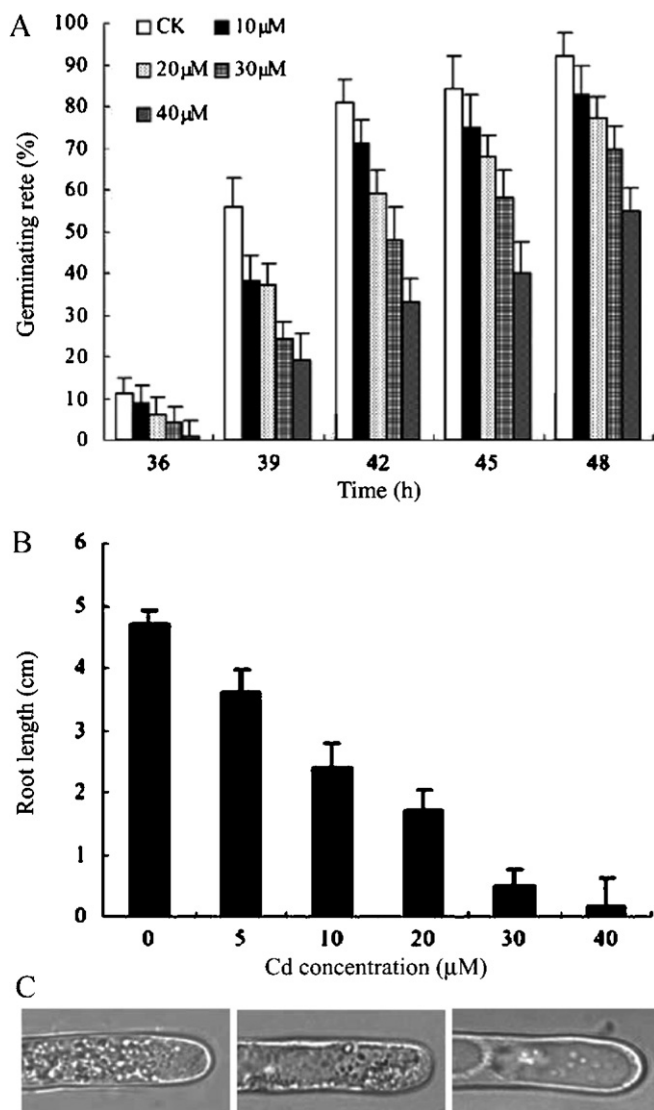


Fig. 1. Effects of CdCl₂ on seed germination and root growth in *Arabidopsis thaliana*. Seed germination and root elongation were inhibited in a dose-dependent manner. (A) Seed germination in the presence of different concentrations of CdCl₂. With increasing CdCl₂ concentrations, seed germination decreased markedly. (B) Root length in the presence of different concentrations of CdCl₂. With increasing CdCl₂ concentrations, root elongation was significantly inhibited. Values are means ± SD. (C) Cytoplasmic architecture of root hairs. *Left*: control cells; *Middle*: root hairs treated with 20 μM CdCl₂; *Right*: root hair treated with 40 μM CdCl₂.

phosphate buffer (pH 7.2); then washed four times for 15 min each time in 100 mM phosphate buffer (pH 7.2); and post-fixed overnight at 4 °C in 1% osmium tetroxide in 100 mM phosphate buffer (pH 7.2). After four washes of 10 min each in 100 mM phosphate buffer (pH 7.2), tissue was dehydrated through an ethanol series (50–100%) for 15 min each at room temperature, and finally embedded in Spurr's resin. Sections were cut using an LKB-V ultramicrotome, and examined with a JEM-1230 electron microscope (Jeol Ltd., Tokyo, Japan).

Results

Seed germination and root growth

The seed germination rate, root growth, and morphological changes in root hairs in *Arabidopsis thaliana* depended on CdCl₂ concentration and time of application (Fig. 1). Seed germination

and root growth were markedly delayed by CdCl₂ in a dose- and time-dependent manner. Seeds started to germinate after 36 h and reached maximum germination percentage at 48 h (Fig. 1A). In controls, the highest germination rate was 92% after 48 h, but these levels were reduced to 9.8%, 16.3%, 23.8%, and 40.2% at different concentrations of CdCl₂ compared to the control (Fig. 1A). Furthermore, CdCl₂ also consistently inhibited primary root elongation (Fig. 1B). Various concentrations of CdCl₂ resulted in root length reductions of 22.5–95.6%, and nearly no root elongation was observed with 40 μM CdCl₂.

Under light microscopy, control root hairs exhibited a typical “clear cap” at the tip, an area lacking microscopically visible organelles (Fig. 1C). On the other hand, root hairs cultured in media containing CdCl₂ showed some abnormalities, such as cytoplasmic vacuolation and a slightly swollen tip. For example, after treatment with 20 μM CdCl₂, the clear zone at the tip of the root hair retracted and was invaded by vacuoles of various sizes, followed by a single large vacuole. When exposed to 40 μM CdCl₂, this zone was completely filled by a large vacuole, indicating that the hair cell had changed from a growing to a non-growing region.

CdCl₂ affects the cytoplasmic Ca²⁺ gradient and extracellular Ca²⁺ flux at the root hair tip

Because of the chemical similarity between Cd and Ca, the latter plays a critical role in polarized tip growth of root hairs, whereas Cd interferes with Ca uptake and Ca signalling in plant cells (Garnier et al., 2006). Therefore, we proposed that CdCl₂ treatment would disrupt Ca homeostasis in root hairs. To examine this hypothesis, cytosolic Ca levels in control and Cd-treated root hairs were compared using Fluo-4/AM dye, which is a Ca-sensitive fluorescent probe used to measure activities of cytoplasmic free Ca ions (Leshem et al., 2006). As shown in Fig. 2, the control root hair showed strong intracellular green fluorescence along its longitudinal axis and selective enrichment of active Ca²⁺ in the root tips (Fig. 2A). Thus, a steep gradient of [Ca²⁺]_{cyt} was seen from the tip to the base in untreated root hairs. Upon CdCl₂ exposure, the fluorescence appeared to be significantly attenuated in both the extreme apex and the shank of the root hairs, and when CdCl₂ concentration was increased to 40 μM, the tip-focused pattern of Ca²⁺ distribution dissipated completely (Fig. 2B and C). To investigate whether this decrease of the fluorescence density resulted from the decreased accumulation of Fluo-4/AM dye due to the vacuolation in the tip of CdCl₂-treated hairs, we observed the cytoplasmic streaming in CdCl₂-treated hairs. As shown in Movies S1–S3, the cytoplasmic streaming remained active in Cd-treated hair cells, suggesting that these cells kept alive and Fluo-4/AM dye should be transported everywhere by diffusing or cytoplasmic streaming.

Using the vibrating electrode technique, we measured Ca²⁺ flux at the extreme apex of root hairs (Fig. 2D–F). Influx of extracellular Ca²⁺ prevailed in normal root hairs (Fig. 2D), but was clearly inhibited after addition of CdCl₂. Upon 20 μM CdCl₂ treatment, the Ca²⁺ influx was nearly unchanged with a range from 93.08 to 188.90 pmol cm⁻² s⁻¹ (mean 105.73 ± 30.50 pmol cm⁻² s⁻¹, n = 10), in comparison to that of control root hair cells (range 45–117 pmol cm⁻² s⁻¹, mean 100.77 ± 3.48 pmol cm⁻² s⁻¹, n = 10). However, the Ca²⁺ efflux was clearly increased with a range from 94.03 to 191.84 pmol cm⁻² s⁻¹ (mean 112.91 ± 36.72 pmol cm⁻² s⁻¹, n = 10), which was wider than that of control root hairs (range 43–57 pmol cm⁻² s⁻¹; mean 51.24 ± 1.51 pmol cm⁻² s⁻¹, n = 10) (Fig. 2E). When the concentration of CdCl₂ was increased to 40 μM, Ca²⁺ influx obviously decreased and showed a narrow flux range from about 77.85 to 79.49 pmol cm⁻² s⁻¹ (mean 78.4 ± 0.53 pmol cm⁻² s⁻¹, n = 10) in comparison to that of either the control or 20 μM CdCl₂-treated root hair cells. The Ca²⁺ efflux with a range from 77 to

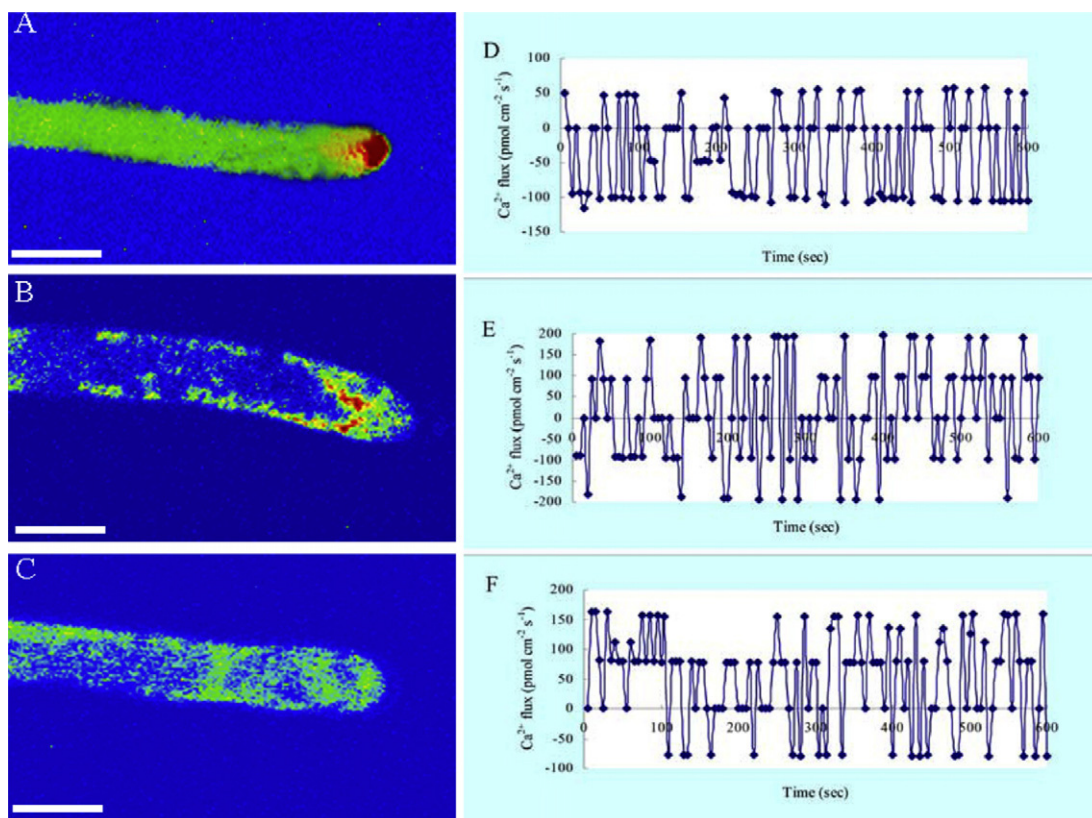


Fig. 2. Rapid changes in $[Ca^{2+}]_{cyt}$ (A–C) and extracellular Ca^{2+} flux (E–F) in response to $CdCl_2$ treatment. (A) Control root hair showed strong fluorescence along the intact root hair and a clear tip-focused Ca gradient. (B) Root hair treated with $20 \mu M CdCl_2$ had a negligible Ca gradient. (C) Root hair treated with $40 \mu M CdCl_2$ showed weak fluorescence, indicating disruption of the Ca gradient. Corresponding bright field images are shown at a reduced size. Bars = $20 \mu m$. (D) Influx of extracellular Ca^{2+} prevailed in control root hairs. (E) Root hairs treated with $20 \mu M CdCl_2$ showed inhibition of Ca^{2+} influx and enhanced Ca^{2+} efflux. (F) Root hairs treated with $40 \mu M CdCl_2$ displayed greater inhibition of Ca^{2+} influx and enhanced Ca^{2+} efflux than those treated with $20 \mu M CdCl_2$.

$164 \text{ pmol cm}^{-2} \text{ s}^{-1}$ (mean $106.99 \pm 12.02 \text{ pmol cm}^{-2} \text{ s}^{-1}$, $n = 10$) was similar to that of $20 \mu M CdCl_2$ -treated root hair cells (Fig. 2F).

Inhibitory effects of $CdCl_2$ on actin polymerization and organization

Changes in plant polarized cell growth have previously been associated with AF reorganization. To determine whether $CdCl_2$ -induced suppression of root growth resulted from disorganization in the actin cytoskeleton, transgenic lines expressing the F-actin binding domain (ABD) of the *Arabidopsis* fimbrin AtFIM1 fused to GFP (FABD2-GFP) were used. FABD2-GFP transgenic *Arabidopsis* seedlings appear to have no phenotypic differences from the wild type and have been widely used to analyze actin cytoskeletal organization in *Arabidopsis* lines (Voigt et al., 2005). The short- and long-term effects of $CdCl_2$ on AFs were examined using LSCM. In root hairs of untreated plants, AFs were distributed throughout the whole root hair and several bundles of AFs were observed parallel to the longitudinal axis of the hair cell. The arrangement of AFs in the control was similar to that resulting from use of fluorescein isothiocyanate (FITC)-conjugated phalloidin labelling in bean root hairs (Cordenas et al., 1998). $CdCl_2$ treatment disrupted AFs in a dose- and time-dependent manner. The treatment with $5 \mu M$ and $10 \mu M CdCl_2$ for several minutes to 1 h did not cause obvious alteration of AFs in root hairs except for bundles of AFs stretching into the tip of root hairs (Fig. S1). After treatment with $5 \mu M CdCl_2$ for 2 h, some transverse AFs occurred beneath the cell apex although longitudinal AFs were maintained (Fig. 3B). With increasing $CdCl_2$ concentrations ($10 \mu M CdCl_2$ for 2 h), dense, twisted, and transversally running arrays of AFs were typical fea-

tures, and the longitudinal arrangement of AFs was completely disrupted (Fig. 3C). Root hairs had progressively increased lesions in the actin cytoskeleton with further exposure to $CdCl_2$ ($10 \mu M$ for 20 h) (Fig. 3D). The transverse AFs became more concentrated and the entire root hair seemed to become highly compartmented by these transverse and winding AFs. However, if seeds germinated on solid medium containing $10 \mu M$ or $20 \mu M CdCl_2$ and continuously grew for 3 days, AFs were nearly kept intact and the organization of longitudinal AFs was maintained (Fig. 3E and F).

Effects of $CdCl_2$ on vesicular trafficking dynamics

As in axonal growth, root hair elongation requires the polar movement of vesicles that add the necessary substances and plasma membrane components by fusing to the cell's growing tip. To examine whether $CdCl_2$ treatment influenced endocytosis and membrane recycling in root hairs, we labelled root hairs with the lipophilic dye FM4-64, a reliable marker used for detection of membrane trafficking events in plant cells (Samaj et al., 2006). The uptake of FM4-64 into root hairs followed a strict time course (Fig. 4). When control seedlings were incubated in an FM4-64-containing solution, the dye was internalized immediately. After about 8 min, the whole of the root hair was stained red and internalized endosome-like vesicles formed from the plasma membrane were detectable. With longer FM4-64 application, the dye combined with the plasma membrane, gradually transferred to the cytoplasm, and the number of fluorescent vesicles increased, as reported previously (Ovecka et al., 2005). The characteristic FM4-64 staining reached a stable state in the cytoplasm after 20–25 min of being most apparent in the apical and sub-apical region (Fig. 4A). In

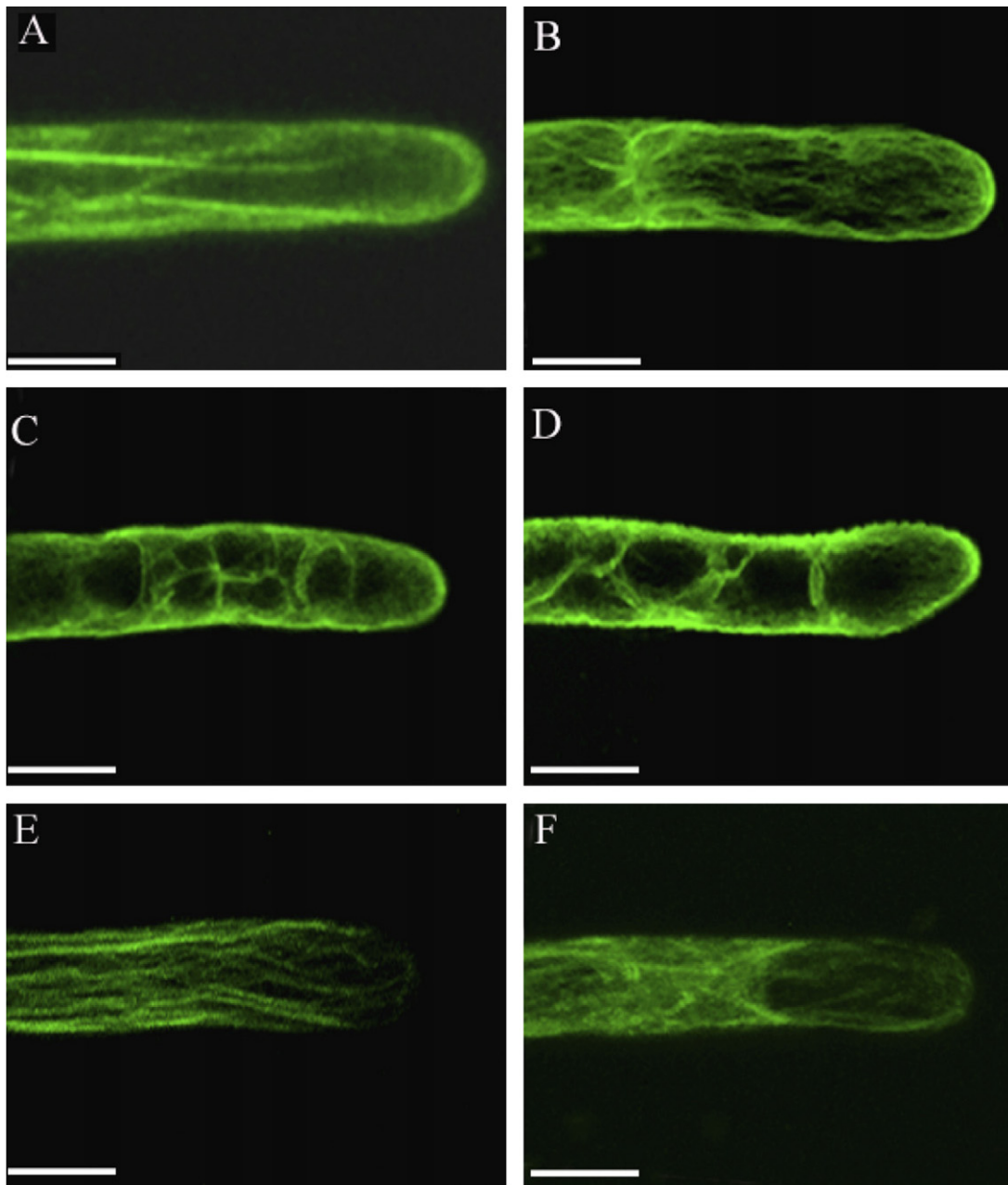


Fig. 3. Distribution of actin filaments (AFs) in root hairs of *Arabidopsis thaliana* after CdCl₂ treatment. (A) Control root hair showing AFs distributed throughout the whole root hair and bundles of AFs mainly parallel to the long axis. (B) Root hair exposed to 5 μM CdCl₂ for 2 h, showing fewer longitudinal AFs and some transverse AFs beneath the cell apex. (C) AFs in root hairs treated with 10 μM CdCl₂ for 2 h appeared localized transversely. (D) Root hair exposed to 10 μM CdCl₂ for 20 h, with longitudinal alignment of AFs completely destroyed and transverse AFs more concentrated. (E) Root hair grown on solid medium containing 10 μM CdCl₂ for 3 days, maintaining longitudinal alignment of AFs except at the apex. (F) Root hair grown on solid medium containing 20 μM CdCl₂ for 3 days, showing longitudinal AFs clearly disrupted throughout. Bars = 10 μm. All figures were projected along the z-axis from 20 to 30 optical serial sections.

contrast, when seedlings were pre-treated with 20 μM CdCl₂ prior to FM4-64 loading, the labelling pattern was distinct from that of the controls (Fig. 4B); few bright, near-spherical structures were detected in the extreme tip when FM4-64 was added for 8 min, and the dye uptake was very slow compared to the controls. Most of the dye remained on/or near the plasma membrane even after a 25-min incubation at room temperature. To test whether CdCl₂ treatment affected the traffic of endocytic vesicles, seedlings were incubated for 5 min in FM4-64-containing medium and transferred into normal growth medium containing 20 μM CdCl₂. Both the untreated and treated root hairs showed strong fluorescence signals at the plasma membrane and in the cytoplasm. No obvious difference was observed in the size of the fluorescent vesicles com-

pared with those in the control hair cells within 1.5 h after CdCl₂ treatment (Fig. S2A and B). The effect of CdCl₂ was detected after 2 h of incubation, when the tonoplast was labelled by FM4-64 dye (Fig. S2C). The fluorescence of FM4-64 in the CdCl₂-treated root hairs remained in the large vesicles and was not present in the tonoplast (Fig. S2D). These data suggest that CdCl₂ inhibits not only the initial stage of endocytosis but also the trafficking of vesicles in the cytoplasm.

Alterations of cell wall components in response to CdCl₂

Because it is well documented that the actin cytoskeleton and vesicle trafficking are closely associated with cell wall formation

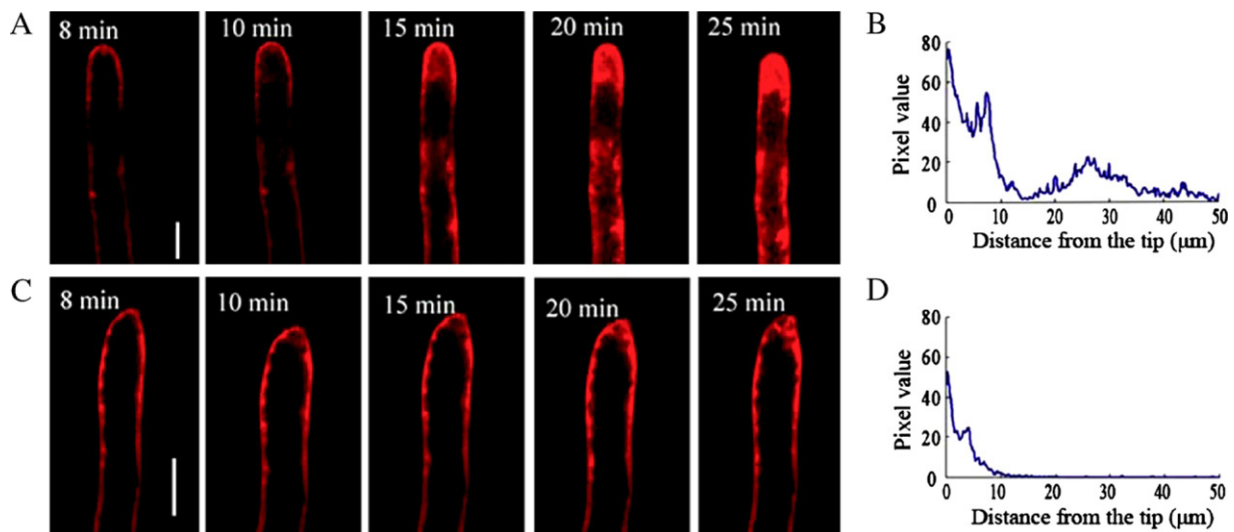


Fig. 4. Time course of FM4-64 uptake in *Arabidopsis thaliana* root hair. (A) FM4-64 staining in control root hair. Uptake of FM4-64 into the cell followed a strict time series and dye uptake took place in the apex and the sub-apical region. (B) Pixel values along a central transect through the fluorescence image in A which was taken after 15-min FM4-64 staining. (C) FM4-64 staining of 20 μM CdCl_2 -treated root hair. The velocity of dye uptake is very slow and most dye remained on or near the plasma membrane after about 25 min. (D) Pixel values along a central transect through the fluorescence image in C which was taken after 15-minute FM4-64 staining. Bars = 10 μm .

(Chen et al., 2007; Bove et al., 2008), we wondered whether CdCl_2 treatment would alter components of the cell wall, resulting in cessation of root hair tip growth. To examine this hypothesis, immunolabelling, fluorescence staining, and FTIR analysis were applied to analyze changes in cell wall components upon CdCl_2 treatment. Because the published data show that antibodies against pectin fail to label root hairs of *Arabidopsis* (Willats et al., 2001), we used JIM5 (anti-de-esterified pectin antibody) and JIM7 (anti-esterified pectin antibody) to detect pectin distribution in radicals. In the control radicals, de-esterified pectin was found on the root surface, but the fluorescence signal was faint in the apical region (Fig. 5A). After 20 μM CdCl_2 treatment, only weak and clustered signals were found in the sub-apical root region (Fig. 5B), and after 40 μM CdCl_2 we were unable to find any fluorescence in the apical and subapical zones (Fig. 5C). Similar to de-esterified pectin, esterified pectin was distributed along the root in the control (Fig. 5D),

and there was no fluorescence in the root tip after treatment with 20 μM CdCl_2 (Fig. 5E). However, dissimilar to de-esterified pectin, esterified pectin appeared dispersed in the intact root upon 40 μM CdCl_2 treatment (Fig. 5F).

In untreated cells, the distribution of cellulose was relatively homogeneous, without any specific deposition in the cell wall, from the trichoblast to the growing tip, after calcofluor labelling (Fig. 6A). Root hairs treated with CdCl_2 showed a different deposition pattern of cellulose along the root hair and calcofluor fluorescence was inclined to focus at the growing tip of 20 μM CdCl_2 -treated root hairs (Fig. 6B). When the concentration of CdCl_2 was increased to 40 μM , cellulose preferentially located at the extreme tip and its content increased, as shown by the more pronounced fluorescence compared with that in control hair cells. Very weak or almost no labelling with calcofluor occurred in other parts of the root hair (Fig. 6C).

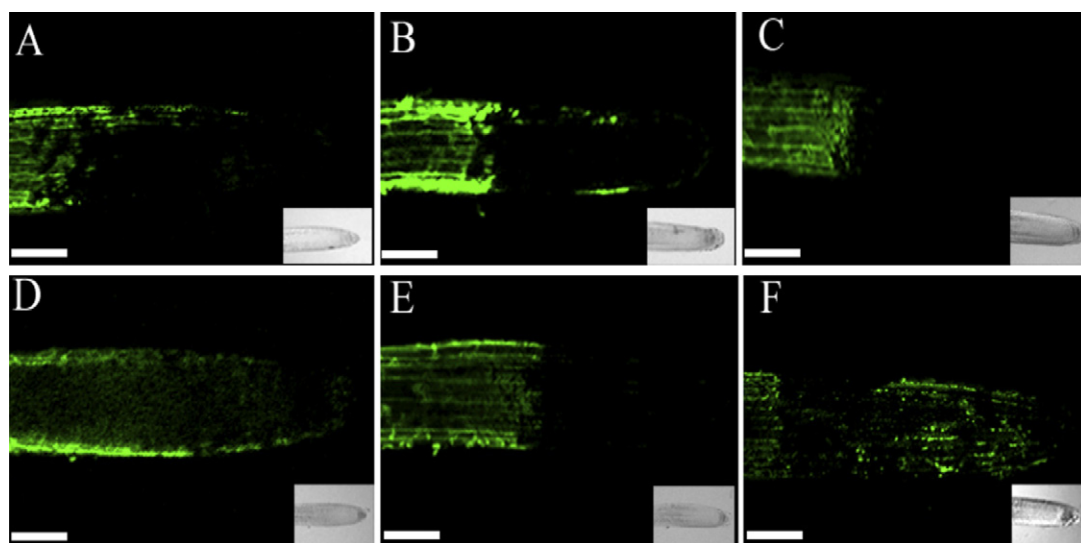


Fig. 5. Effects of CdCl_2 on pectins in roots. (A) JIM5 (anti-de-esterified pectin antibody) labelling of control root showing that fluorescence occurred along the entire root, but the signal is faint in the apical region. (B) JIM5 labelling of root treated with 20 μM CdCl_2 showing weak and clustered signals in the sub-apical region. (C) JIM5 labelling of root treated with 40 μM CdCl_2 showing no signal in the apical and sub-apical zones. (D) JIM7 (anti-esterified pectin antibody) labelling of control root showing a similar labelling pattern to JIM5. (E) JIM7 labelling of root exposed to 20 μM CdCl_2 showing no fluorescence in the root tip. (F) JIM7 labelling of root treated with 40 μM CdCl_2 showing sporadic distribution along the root. Bars = 10 μm .

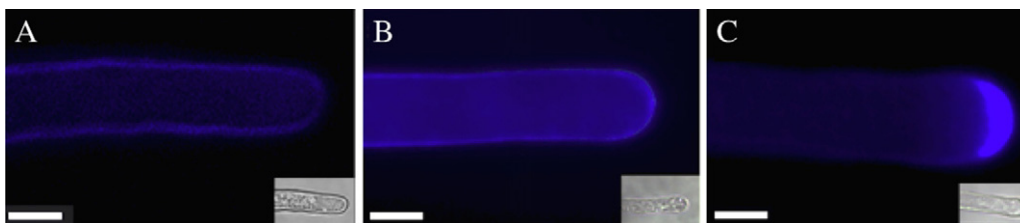


Fig. 6. Effects of CdCl₂ on cellulose in root hairs. (A) Control root hair with relatively homogeneous cellulose distribution throughout the cell wall. (B) Root hair treated with 20 μM CdCl₂ showing a tip-locating inclination of cellulose. (C) Root hair treated with 40 μM CdCl₂ with cellulose preferentially located at the extreme tip. Corresponding bright field images are shown at a reduced size. Bars = 10 μm.

FTIR spectroscopy is a direct and non-destructive technique method for qualitative and quantitative analysis of various biopolymers in plant cell walls (Brown et al., 2005; Mouille et al., 2006). The validity and sensitivity of the method have been demonstrated in the screening assays of *Arabidopsis* mutants defective in cell wall materials (Chen et al., 1998; Mouille et al., 2003; Brown et al., 2005). Typical FTIR spectra were collected from the tip region of root hair. The number and the pattern of the peaks obtained from the CdCl₂-treated root hairs were indistinguishable from the control. Several distinct peaks corresponding to esterified pectins (1740 cm⁻¹), de-esterified pectins (1600 cm⁻¹), proteins (1650 and 1550 cm⁻¹; amide I and amide II) and other polysaccharides (1200–900 cm⁻¹) were found (Fig. 7A). To obtain information about the effects of CdCl₂ on the spectral differences, differential spectrums were generated by the digital subtraction of the control from the spectrum of

CdCl₂-treated root hairs. As shown in Fig. 7B, the esterified pectin peak was slightly weaker, but the de-esterified pectin peak was relatively stronger when compared with that in control cells. Furthermore, peaks designated as proteins and some polysaccharides were observed in a difference spectrum, showing that there were more proteins and polysaccharides in CdCl₂-exposed root hairs than that in the untreated hair cells.

CdCl₂ disrupts the ultrastructure of organelles and induces vacuolization in root cells

Control root cells examined by transmission electron microscopy (TEM) had relatively thick cytoplasm (Fig. 8A and B) and large organelles such as mitochondria and endoplasmic reticulum (ER) and a large central vacuole (Fig. 8C–E). Mitochondria were nearly spherical and possessed numerous well-developed cristae and an electron-dense matrix. The ER cisternae were mostly flat with uniform intra-cisternal spacing between the limiting membranes and were studded with a large amount of ribosomes. Much variation was observed in root cells treated with CdCl₂ (Fig. 8F–O), depending on concentration used. The most obvious change was vacuolization of the cytoplasm, as shown by an increase in the number of vacuoles of varied sizes. After treatment with 20 μM CdCl₂, the cytoplasm appeared thinner than that in the control cells and a number of small vacuoles appeared (Fig. 8F and G). Wider, variable intra-cisternal spaces of ER cisternae were recognized, although some ribosomes were still present on the surfaces of the ER membrane (Fig. 8H, I). Mitochondria were slightly dilated and their cristae were blurred (Fig. 8J). Increasing the CdCl₂ concentration to 40 μM induced vacuolization of a greater proportion of root cells and a remarkable extension of the vacuolar system into the plasma membrane (Fig. 8K and M). Mitochondria became more swollen and irregular, internal membranes began to degrade, and the structure of the cristae was disrupted (Fig. 8L, N, and O).

Discussion

Cd is one of the most toxic heavy metals and seriously inhibits plant growth (Zhang et al., 2005), consistent with the results presented here. In our investigation, the addition of CdCl₂ severely inhibited germination and root elongation in a dose-dependent manner. The inhibitory effects of CdCl₂ were also apparent in the cytoplasmic architecture of root hairs: the clear zone at the root hair tip disintegrated and subsequently was protruded with varied sizes of vacuoles. This aberration in the root hair tip may have been mediated by alterations of the cytosolic tip-focused Ca²⁺ gradient and/or polarized actin organization, both of which provide spatial information for maintaining the clear zone and tip growth (Wymer et al., 1997; Chen et al., 2007), as discussed below.

Calcium ions serve as a second messenger in a variety of plant physiological processes. In root hairs, the existence of a tip-to-base concentration gradient of cytosolic Ca²⁺ is essential for tip growth

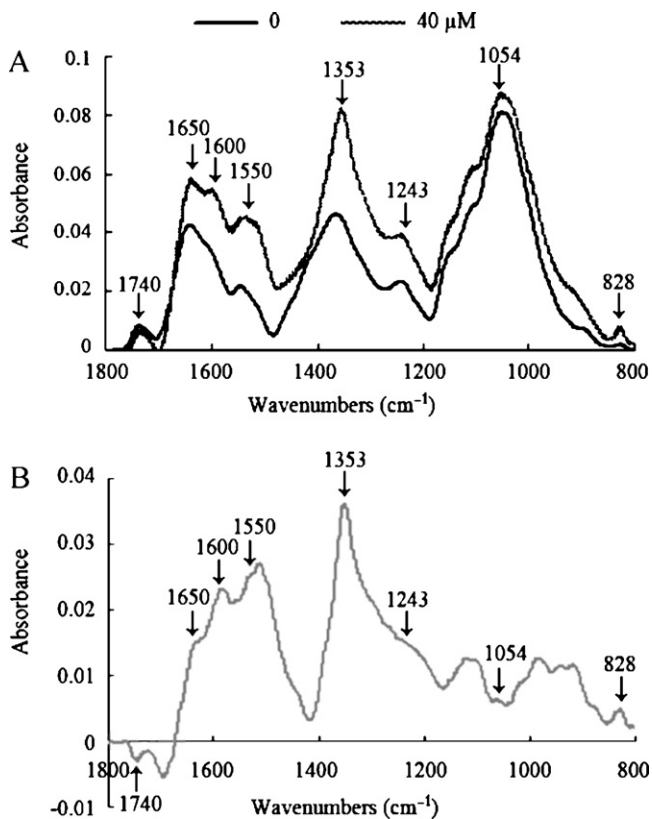


Fig. 7. Fourier transform infrared (FTIR) microspectroscopic spectra obtained from the apical region of *Arabidopsis thaliana* root hairs. (A) FTIR spectra from the tip region of untreated (control) and 40 μM CdCl₂-treated root hairs. Esterified pectin and de-esterified peaks were detected at 1740 and 1600 cm⁻¹, respectively, proteins were detected at 1650 and 1550 cm⁻¹. (B) The different spectra generated by digital subtraction of the control spectra from the spectra of CdCl₂-treated root hair walls showing the decreased content of esterified pectins and the increase in acidic pectins, proteins, and other polysaccharides.

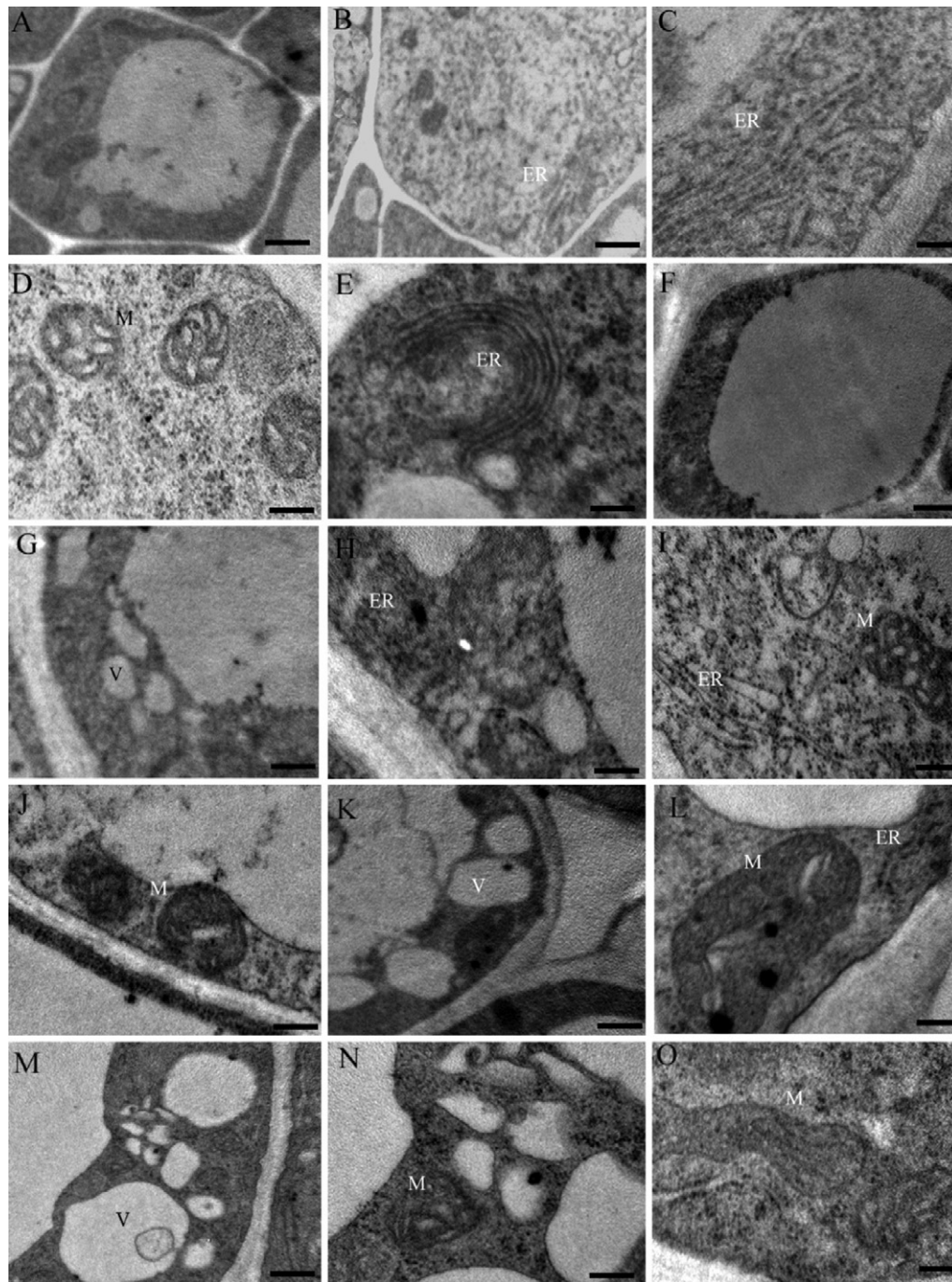


Fig. 8. Electron micrographs of control and CdCl₂-treated root meristematic cells of 3-day-old seedling. (A–E) Ultrastructure of cells in control root showing normal cytoplasm (A, bar = 2 μm) and organelles (B, C and E, bars = 0.2 μm). (F–J) Root cells treated with 20 μM CdCl₂ appeared thinner cytoplasm (F, bar = 0.5 μm), a number of small vacuoles (G, bar = 1 μm), wider and more variable intra-cisternal spaces of ER cisternae (H and I, bars = 0.2 μm), and slightly dilated mitochondria and blurred cristae (J, bar = 0.2 μm). (K–O) Higher concentrations (40 μM) of CdCl₂ induced vacuolation (K, bar = 1 μm), more swollen and irregular mitochondria (L, bar = 0.5 μm), a remarkable extension of the vacuolar system into the plasma membrane (M, bar = 2 μm) and the disruption of internal membrane of the mitochondria and cristae in root cells (N and O, bars = 0.2 μm).

(Mathur and Hulskamp, 2001). Treatments with auxin, dibromo-BAPTA or La³⁺, which can destroy or diminish this gradient, lead to the cessation of tip growth (Felle and Hepler, 1997; Carol and Dolan, 2002). Furthermore, if these treatments did not considerably decrease [Ca²⁺]_{cyt} in the tip of root hairs, the polar growth was hardly affected (Felle and Hepler, 1997), suggesting that the dissipation of Ca²⁺ gradient is probably the cause but not the consequence of the growth inhibition under the treatments that disturb Ca²⁺ gradient. Because of identical charges and similar ionic radii between Cd²⁺ and Ca²⁺, Cd²⁺ may interfere with the biological

activity of Ca²⁺ by entering cells through Ca²⁺-selective channels (Perfus-Barbeoch et al., 2002). Clemens et al. (1998) reported that Ca²⁺ uptake activity of the wheat transporter LTC1 (a non-selective transmembrane transporter) was blocked by Cd. Other studies have documented that Cd often reduces the uptake of Ca²⁺, decreases the concentration of Ca²⁺ in tissue, and consequently causes Ca²⁺ deficiency (Perfus-Barbeoch et al., 2002). However, CdCl₂ treatment did not induce an increase in Ca²⁺ influx in BY-2 cells (Garnier et al., 2006), in agreement with our results from the vibrating electrode assay, which showed that Ca²⁺ influx was

inhibited and Ca^{2+} efflux enhanced at the extreme apex of root hairs treated with CdCl_2 for 600 s. Furthermore, the fluctuation of $[\text{Ca}^{2+}]_{\text{cyt}}$ is dependent on not only extracellular Ca^{2+} influx but also the release of Ca^{2+} from intracellular Ca pools. However, TEM showed that the structure of intracellular Ca^{2+} pools, such as in mitochondria and ER, was destroyed in roots upon CdCl_2 exposure. This indicates that the significant changes in intracellular fluorescence intensity of Ca^{2+} and dissipation of the tip-focused Ca^{2+} gradient in Cd-treated root hairs might be a consequence of the lack or effusion of internal Ca^{2+} and a decrease of extracellular Ca^{2+} influx.

It is well known that the actin cytoskeleton has a pivotal role in maintenance of elongation in tip-growing plant cells. Treatment with latrunculin B, an inhibitor of actin polymerization, resulted in inhibition of tip growth in *Arabidopsis* and maize root hairs (Baluska et al., 2000) and pollen tubes (Chen et al., 2007). This result was confirmed by genetic studies. Mutations in ACTIN2 (ACT2), a member of the *Arabidopsis* actin family, caused a hairless or short-hair phenotype that was swollen in shape (Ringli et al., 2002). The results of the present study showed marked disruption of AFs in a dose- and time-dependent manner after CdCl_2 treatment. As little as $5 \mu\text{M}$ CdCl_2 disrupted the distribution of AFs, changing them from a longitudinal to a transverse array. With increasing CdCl_2 concentrations, longitudinal AFs completely disappeared and the entire root hair became compartmented by transverse and winding AFs. This is consistent with results from green alga *Spirogyra decimina* and from several kinds of animal cells (Prozialeck and Niewenhuis, 1991; Wang and Templeton, 1996; Pribyl et al., 2005). Elsewhere, it was reported that Ca^{2+} was intimately connected with the organization of AFs, with increase of Ca^{2+} concentration resulting in destabilization and depolymerization of actin (Khaitlina and Hinssen, 2002; Zhang et al., 2010). However, in the present study, the cytoplasmic Ca^{2+} decreased together with the disorganization of AFs in CdCl_2 -treated root hairs. The most probable explanation for this phenomenon is that Cd^{2+} might mimic Ca^{2+} to activate AF-severing proteins and thus lead to AFs depolymerization. It has been reported that Cd^{2+} can substitute for Ca^{2+} in the crystal structure of gelsolin, a calcium-dependent actin-severing protein, at a Ca^{2+} -binding site in domain 2, and then activate gelsolin for AF binding and severing (Kazmirski et al., 2002). Apostolova et al. (2006) found that Cd can activate the association of gelsolin with actin cytoskeleton, with gelsolin's severing properties. Therefore it is possible that Cd^{2+} activates one or several certain actin-severing proteins by substituting directly for Ca^{2+} , or alternatively by displacing Ca^{2+} from other cellular sites and making it available to these proteins in cells (Suzuki et al., 1985; Apostolova et al., 2006). Based on these results, it is suggested that Cd^{2+} -induced AF disruption relates to the inhibition of tip growth of CdCl_2 -treated root hairs.

The strong inhibitory effects of CdCl_2 on root growth may be mediated by its role in vesicular trafficking, which is essential for establishing and maintaining polarity in root hairs. Time-lapse images of CdCl_2 -treated root hairs showed a distinct FM dye staining pattern from that of control cells, suggesting that membrane endocytosis and vesicular trafficking were perturbed during CdCl_2 stress. This effect of CdCl_2 on endocytosis and vesicular trafficking in root hairs is different from recently published data showing that internalization of FM4-64 was induced in root cells under salt stress (Leshem et al., 2007). The difference may be due to a difference in environmental stimulus applied (CdCl_2 versus NaCl) or in the cell types observed (root hair cells versus other root cells). It is well accepted that Ca^{2+} has a profound effect on the organization of AFs and the oriented transport of vesicles toward the cell wall in cells, especially in polarized cells (Roy et al., 1999). Our results showed that CdCl_2 treatment slowed vesicle trafficking, accompanied by a dissipation of the Ca^{2+} gradient and depolymerization of AFs in root hairs (Figs. 2 and 3). This implies that vesicular traf-

ficking in the tip region of root hairs is partly dependent on the Ca^{2+} gradient and AF arrangement during CdCl_2 treatment in root hairs.

The plant cell wall is a dynamic structure that is mostly composed of cellulose fibres embedded in a gel of pectin and includes a variety of glycans and proteins. Cellulose is composed of hydrogen-bonded beta-1,4-linked glucan chains that are synthesized at the plasma membrane by large cellulose synthase (CESA) complexes. In contrast, pectin, hemicellulose, and other carbohydrate polymers are synthesized within the Golgi apparatus and then exported to the surface to assemble with cellulose to form the cell wall (Willats et al., 2001). Numerous proteins are also secreted via the Golgi and are thought to be complexed with the carbohydrate components of the wall at the cell surface (Kohorn et al., 2000). Therefore, vesicular trafficking involved in the secretory process is intimately associated with the deposition of cell wall components. In our study, immunolabelling with JIM5 and JIM7 gave no detectable signals on the surface of root hairs, whereas FTIR analyzes revealed that both de-esterified and esterified pectins were present in hair cells, indicating that these two types of pectin epitope might be masked by other wall components, such as hydroxyproline-rich glycoproteins (HRGPs), as reported by Willats et al. (2001). This is inconsistent with the results obtained by Sherrier and Vandebosch (1994), in which both pectins were detected in the cell wall of *Vicia* root hairs by immunolabelling with JIM5 and JIM7. Compared to root hairs, JIM5 and JIM7 produced intense labelling of the radial surface apart from the apex, where only sporadic spots were observed. This is similar to the labelling pattern of lateral roots, but inconsistent with that of radicals of 10- to 15-day-old *Arabidopsis* seedlings using JIM5 and JIM7. This suggests that pectin epitopes are differently regulated at different developmental stages – being abundant on the older rather than the younger (3-day) radical apex (Willats et al., 2001). In response to CdCl_2 treatment, the distribution of both types of pectin on the radical apex differed with different CdCl_2 concentrations, indicating that CdCl_2 spatially modulates the synthesis and distribution of de-esterified and esterified pectins. In addition, de-esterified pectins can bind with Ca by their carboxyl groups and thus increase stiffening of cell wall, which markedly inhibits cell elongation (Taylor and Hepler, 1997; O'Neill et al., 2004). We found that de-esterified pectins markedly accumulated while esterified pectins decreased in the CdCl_2 -treated root hairs. Other polysaccharides and components in the cell wall such as cellulose, semi-cellulose and proteins also play a crucial role in metal binding and accumulation. Douchiche et al. (2007) found Cd treatment induced the increase of the amount of cellulose. Moreover, negatively charged cellulose and cellulose derivatives bind with Cd in mycorrhizal fungi after CdCl_2 treatment (González-Guerrero et al., 2008). In the present study, the level and distribution pattern of cellulose obtained by FTIR analysis and immunolabelling showed that CdCl_2 preferentially induced the deposition of cellulose in the apical dome of CdCl_2 -treated roots, suggesting that constraint of CdCl_2 by excess cellulose may partly account for detoxification of CdCl_2 in the tip zone of root hairs. Previous studies have documented that cellulose synthase (CESA) is assembled in the Golgi and then exported to the plasma membrane via exocytosis and disorganization of AFs alters the conformation of CESA and prevents correctly patterned deposition of cellulose in the cell wall (Mutwil et al., 2008; Wightman and Turner, 2008). Therefore, it can be hypothesized that treatment with CdCl_2 might trigger an alteration in the orientation of vesicular trafficking because of disorganization of AFs and result in variation of the spatial distribution and contents of pectin and cellulose in *Arabidopsis* roots.

In summary, our investigation into the effects of CdCl_2 on *A. thaliana* roots, especially root hairs, provides evidence of the cytotoxicity of CdCl_2 in polarized tip growth of root hairs. Disruption

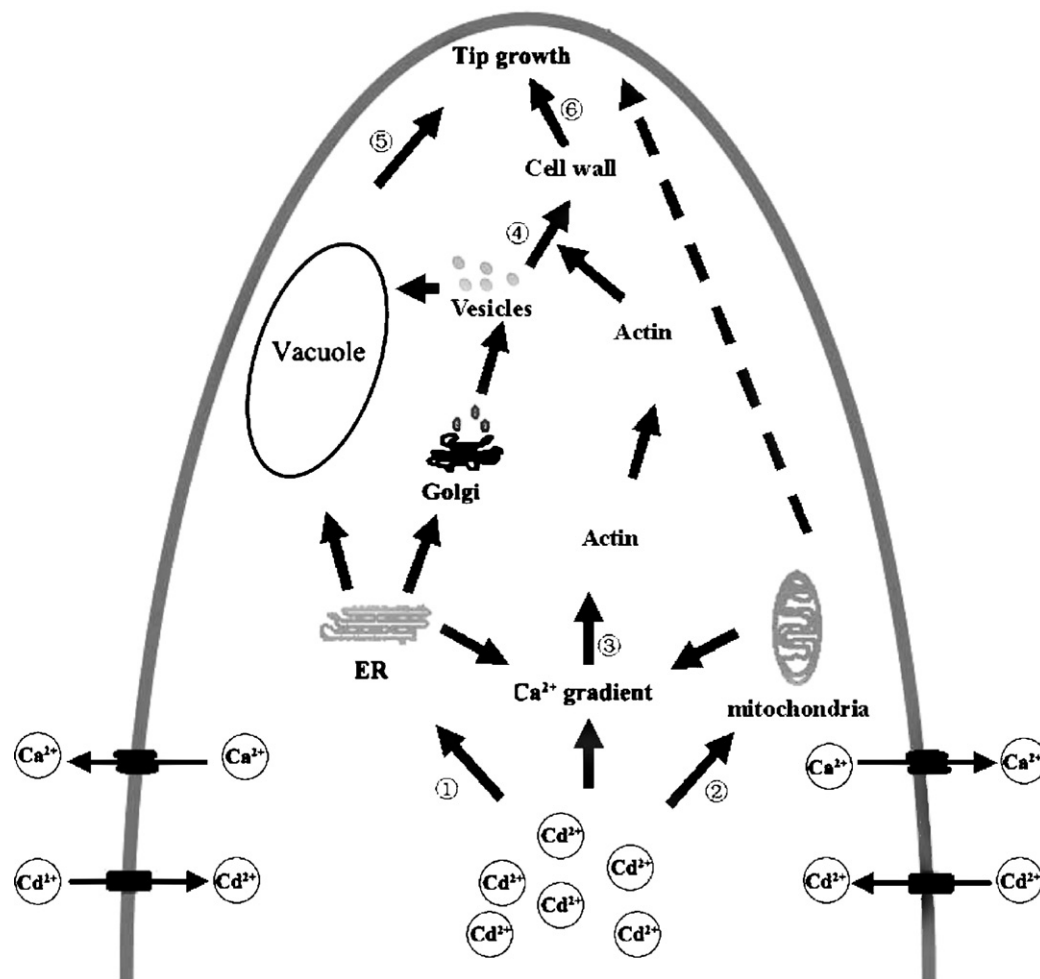


Fig. 9. Hypothetical model showing summarizing main effects of CdCl₂ treatment on the tip growth of *Arabidopsis* root hair. Cd entered the cell through a still unidentified metal transporter (?) or Ca²⁺ channels (■) by mimicking Ca²⁺ ions. Disruption of the structure of ER (1) and mitochondria (2) and enhancement of Ca²⁺ efflux lead to Ca²⁺ gradient dissipation, which causes disorganization of actin filaments (3) in root hairs. Consequently, inhibition of vesicular trafficking (4) results in the alterations of cell wall components. Simultaneous vacuolization (5) and impairment of cell wall (6) lead to the disturbing of tip growth.

of the structure of ER and mitochondria and enhancement of Ca²⁺ efflux by CdCl₂ result in Ca²⁺ gradient dissipation, which causes disassembling of AFs in root hairs. Consequently, change of vesicular trafficking, disorganization of the cell wall, and cytoplasmic vacuolization lead to the disturbance of tip growth, which are summarized in Fig. 9. Therefore, our data provides the mechanistic framework for the cytological effects of CdCl₂ treatment on the tip growth of *A. thaliana* root hairs.

Acknowledgements

This work was funded by the National Natural Science Foundation of China (NSFC) (Nos. 30770123 and 90817010), the National High Technology Research and Development Program of China (863 Program) (No. 2008AA10Z130) and the Knowledge Innovation Program of the Chinese Academy of Sciences (No. KJXC2-YW-L08). We thank Dr. Shanjin Huang (Institute of Botany, CAS, China) for kindly providing FABD2-GFP transgenic *Arabidopsis* seeds.

Appendix A. Supplementary data

Supplementary data associated with this article can be found, in the online version, at 10.1016/j.jplph.2011.01.031.

References

Apostolova MD, Christova T, Templeton DM. Involvement of gelsolin in cadmium-induced disruption of the mesangial cell cytoskeleton. *Toxicol Sci* 2006;89:465–74.

Baluska F, Salaj J, Mathur J, Braun M, Jasper F, Samaj J, et al. Root hair formation: F-actin-dependent tip growth is initiated by local assembly of profilin-supported F-actin meshworks accumulated within expansin-enriched bulges. *Dev Biol* 2000;227:618–32.

Bove J, Vaillancourt B, Kroeger J, Hepler PK, Wiseman PW, Geitmann A. Magnitude and direction of vesicle dynamics in growing pollen tubes using spatiotemporal image correlation spectroscopy and fluorescence recovery after photobleaching. *Plant Physiol* 2008;147:1646–58.

Brown DM, Zeef LAH, Ellis J, Goodacre R, Turner SR. Identification of novel genes in *Arabidopsis* involved in secondary cell wall formation using expression profiling and reverse genetics. *Plant Cell* 2005;17:2281–95.

Carol RJ, Dolan L. Building a hair: tip growth in *Arabidopsis thaliana* root hairs. *Philos Trans R Soc Lond B Biol Sci* 2002;357:815–21.

Chaoui A, El Ferjani E. Effects of cadmium and copper on antioxidant capacities, lignification and auxin degradation in leaves of pea (*Pisum sativum* L.) seedlings. *C R Biol* 2005;328:23–31.

Chen L, Carpita NC, Reiter WD, Wilson RH, Jeffries C, McCann MC. A rapid method to screen for cell-wall mutants using discriminant analysis of Fourier transform infrared spectra. *Plant J* 1998;16:385–92.

Chen T, Teng NJ, Wu XQ, Wang YH, Tang W, Samaj J, et al. Disruption of AFs by latrunculin B affects cell wall construction in *Picea meyeri* pollen tube by disturbing vesicle trafficking. *Plant Cell Physiol* 2007;48:19–30.

Clemens S, Antosiewicz DM, Ward JM, Schachtman DP, Schroeder JI. The plant cDNA LCT1 mediates the uptake of calcium and cadmium in yeast. *Proc Natl Acad Sci* 1998;95:12043–8.

Crdenas L, Vidali L, Domnguez J, Prez H, Snchez F, Hepler PK, et al. Rearrangement of actin microfilaments in plant root hairs responding to *rhizobium etli* nodulation signals. *Plant Physiol* 1998;116:871–7.

- Douchiche O, Rihouey C, Schaumann A, Driouich A, Morvan C. Cadmium-induced alterations of the structural features of pectins in flax hypocotyl. *Planta* 2007;225:1301–12.
- Felle HH, Hepler PK. The Cytosolic Ca²⁺ Concentration gradient of *Sinapis alba* root hairs as revealed by Ca²⁺-selective microelectrode tests and Fura-Dextran ratio imaging. *Plant Physiol* 1997;114:39–45.
- García-Ríos V, Freile-Pelegrin Y, Robledo D, Mendoza-Cozatl D, Moreno-Sánchez R, Gold-Bouchot G. Cell wall composition affects Cd²⁺ accumulation and intracellular thiol peptides in marine red algae. *Aquat Toxicol* 2007;81:65–72.
- Garnier L, Simon-Plas F, Thuleau P, Agnel JP, Blein JP, Ranjeva R, et al. Cadmium affects tobacco cells by a series of three waves of reactive oxygen species that contribute to cytotoxicity. *Plant Cell Environ* 2006;29:1956–69.
- González-Guerrero M, Melville LH, Ferrol N, Lott JN, Azcón-Aguilar C, Peterson RL. Ultrastructural localization of heavy metals in the extraradical mycelium and spores of the arbuscular mycorrhizal fungus *Glomus intraradices*. *Can J Microbiol* 2008;54:103–10.
- Hall JL. Cellular mechanisms for heavy metal detoxification and tolerance. *J Exp Bot* 2002;53:1–11.
- Halperin SJ, Gilroy S, Lynch JP. Sodium chloride reduces growth and cytosolic calcium, but does not affect cytosolic pH, in root hairs of *Arabidopsis thaliana* L. *J Exp Bot* 2003;54:1269–80.
- Holdaway-Clarke TL, Feijo JA, Hackett GR, Kunkel JG, Hepler PK. Pollen tube growth and the intracellular cytosolic calcium gradient oscillate in phase while extracellular calcium influx is delayed. *Plant Cell* 1997;9:1999–2010.
- Kazmirski SL, Isaacson RL, An C, Buckle A, Johnson CM, Daggett V, et al. Loss of a metal-binding site in gelsolin leads to familial amyloidosis. *Nat Struct Biol* 2002;9:112–6.
- Khaitlina S, Hinssen H. Ca-dependent binding of actin to gelsolin. *FEBS Lett* 2002;521:14–8.
- Kohorn BD. Plasma membrane-cell wall contacts. *Plant Physiol* 2000;124:31–8.
- Lee YJ, Szumlanski A, Nielsen E, Yang Z. Rho-GTPase-dependent filamentous actin dynamics coordinate vesicle targeting and exocytosis during tip growth. *J Cell Biol* 2008;181:1155–68.
- Leshem Y, Melamed-Book N, Cagnac O, Ronen G, Nishri Y, Solomon M, et al. Suppression of *Arabidopsis* vesicle-SNARE expression inhibited fusion of H₂O₂-containing vesicles with tonoplast and increased salt tolerance. *Proc Natl Acad Sci* 2006;103:18008–13.
- Leshem Y, Seri L, Levine A. Induction of phosphatidylinositol 3-kinase-mediated endocytosis by salt stress leads to intracellular production of reactive oxygen species and salt tolerance. *Plant J* 2007;51:185–97.
- Mathur J, Hulskamp M. Cell growth: how to grow and where to grow. *Curr Biol* 2001;11:R402–4.
- Mikes J, Siglova M, Cejkova A, Masak J, Jirku V. The influence of heavy metals on the production of extracellular polymer substances in the processes of heavy metal ions elimination. *Water Sci Technol* 2005;52:151–6.
- Mouille G, Robin S, Lecomte M, Pagant S, Hofte H. Classification and identification of *Arabidopsis* cell wall mutants using Fourier-Transform InfraRed (FT-IR) microspectroscopy. *Plant J* 2003;35:393–404.
- Mouille G, Witucka-Wall H, Bruyant MP, Loudet O, Pelletier S, Rihouey C, et al. Quantitative trait loci analysis of primary cell wall composition in *Arabidopsis*. *Plant Physiol* 2006;141:1035–44.
- Mutwil M, Debolt S, Persson S. Cellulose synthesis. A complex complex. *Curr Opin Plant Biol* 2008;11:352–7.
- O'Neill MA, Ishii T, Albersheim P, Darvill AG. Rhamnogalacturonan II: structure and function of a borate cross-linked cell wall pectic polysaccharide. *Annu Rev Plant Biol* 2004;55:9–39.
- Orvar BL, Sangwan V, Omann F, Dhindsa RS. Early steps in cold sensing by plant cells: the role of actin cytoskeleton and membrane fluidity. *Plant J* 2000;23:785–94.
- Ovecka M, Lang I, Baluska F, Ismail A, Illes P, Lichtscheidl IK. Endocytosis and vesicle trafficking during tip growth of root hairs. *Protoplasma* 2005;226:39–54.
- Perfus-Barbeoch L, Leonhardt N, Vavasseur A, Forestier C. Heavy metal toxicity: cadmium permeates through calcium channels and disturbs the plant water status. *Plant J* 2002;32:539–48.
- Powlin SS, Keng PC, Miller RK. Toxicity of cadmium in human trophoblast cells (JAR choriocarcinoma): role of calmodulin and the calmodulin inhibitor, zaldaride maleate. *Toxicol Appl Pharmacol* 1997;144:225–34.
- Pribyl P, Cepák V, Zachleder V. Cytoskeletal alterations in interphase cells of the green alga *Spirogyra decimina* in response to heavy metals exposure. I: The effect of cadmium. *Protoplasma* 2005;226:231–40.
- Prozialek WC, Niewenhuis RJ. Cadmium (Cd²⁺) disrupts Ca²⁺-dependent cell-cell junctions and alters the pattern of E-cadherin immunofluorescence in LLC-PK1 cells. *Biochem Biophys Res Commun* 1991;181:1118–24.
- Raize O, Argaman Y, Yannai S. Mechanisms of biosorption of different heavy metals by brown marine macroalgae. *Biotechnol Bioeng* 2004;87:451–8.
- Ringli C, Baumberg N, Diet A, Frey B, Keller B. ACTIN2 is essential for bulge site selection and tip growth during root hair development of *Arabidopsis*. *Plant Physiol* 2002;129:1464–72.
- Roy SJ, Holdaway-Clarke TL, Hackett GR, Kunkel JG, Lord EM, Hepler PK. Uncoupling secretion and tip growth in lily pollen tubes: evidence for the role of calcium in exocytosis. *Plant J* 1999;19:379–86.
- Samaj J, Müller J, Beck M, Böhm N, Menzel D. Vesicular trafficking, cytoskeleton and signalling in root hairs and pollen tubes. *Trends Plant Sci* 2006;11:594–600.
- Sherrier DJ, VandenBosch KA. Secretion of cell wall polysaccharides in *Vicia* root hairs. *Plant J* 1994;5:185–95.
- Stohs SJ, Bagchi D, Hassoun E, Bagchi M. Oxidative mechanisms in the toxicity of chromium and cadmium ions. *J Environ Pathol Toxicol Oncol* 2000;19:201–13.
- Suzuki Y, Chao S-H, Zysk JR, Cheung WY. Stimulation of calmodulin by cadmium ion. *Arch Toxicol* 1985;57:205–11.
- Taylor LP, Hepler PK. Pollen germination and tube growth. *Annu Rev Plant Physiol Plant Mol Biol* 1997;48:461–91.
- Vassilieva EV, Nusrat A. Vesicular trafficking: molecular tools and targets. *Methods Mol Biol* 2008;440:3–14.
- Verma K, Shekhawat GS, Sharma A, Mehta SK, Sharma V. Cadmium induced oxidative stress and changes in soluble and ionically bound cell wall peroxidase activities in roots of seedling and 3–4 leaf stage plants of *Brassica juncea* (L.) Czern. *Plant Cell Rep* 2008;27:1261–9.
- Voigt B, Timmers AC, Samaj J, Müller J, Baluska F, Menzel D. GFP-FABD2 fusion construct allows *in vivo* visualization of the dynamic actin cytoskeleton in all cells of *Arabidopsis* seedlings. *Eur J Cell Biol* 2005;84:595–608.
- Wang Z, Templeton DM. Cellular factors mediate cadmium-dependent actin depolymerization. *Toxicol Appl Pharmacol* 1996;139:115–21.
- Wightman R, Turner SR. The roles of the cytoskeleton during cellulose deposition at the secondary cell wall. *Plant J* 2008;54:794–805.
- Willats WGT, McCartney L, Knox JP. In situ analysis of pectic polysaccharides in seed mucilage and at the root surface of *Arabidopsis thaliana*. *Planta* 2001;213:37–44.
- Wymer CL, Bibikova TN, Gilroy S. Cytoplasmic free calcium distributions during the development of root hairs of *Arabidopsis thaliana*. *Plant J* 1997;12:427–39.
- Zhang H, Qu X, Bao C, Khurana P, Wang Q, Xie Y, et al. *Arabidopsis* VILLIN5, an actin filament bundling and severing protein, is necessary for normal pollen tube growth. *Plant Cell* 2010;22:2749–67.
- Zhang HY, Jiang YN, He ZY, Ma M. Cadmium accumulation and oxidative burst in garlic (*Allium sativum*). *J Plant Physiol* 2005;162:977–84.
- Zhang WH, Rengel Z, Kuo J. Determination of intracellular Ca²⁺ in cells of intact wheat roots: loading of acetoxymethyl ester of Fluo-3 under low temperature. *Plant J* 1998;15:147–51.